Nucleation and Crystallization in Double Crystalline Poly(*p*-dioxanone)-*b*-poly(ϵ-caprolactone) Diblock Copolymers

J. Albuerne, L. Márquez, and A. J. Müller*

Grupo de Polímeros USB, Departamento de Ciencia de los Materiales, Universidad Simón Bolívar, Apartado 89000, Caracas 1080-A, Venezuela

J. M. Raquez, Ph. Degée, and Ph. Dubois

Laboratory of Polymeric and Composite Materials (LPCM), University of Mons-Hainaut, Place du Parc 20, 7000 Mons, Belgium

V. Castelletto and I. W. Hamley*

Department of Chemistry, University of Leeds, Leeds LS2 9JT, UK

Received October 22, 2002; Revised Manuscript Received January 6, 2003

ABSTRACT: The crystallization behavior of three double crystalline diblock copolymers containing poly(ϵ-caprolactone) and poly(*p*-dioxanone) has been studied via differential scanning calorimetry (DSC), polarized optical microscopy (POM), and wide-angle X-ray scattering (WAXS). Crystallization and melting temperatures and enthalpies are compared among copolymers and to those of the corresponding homopolymers. Only one crystallization exotherm was observed for the diblocks. DSC and WAXS indicated that during isothermal crystallization PPDX crystallized first, followed by PCL. POM revealed a transformation of crystalline morphologies at around 50 °C, from granular aggregates at high temperature (where only PPDX is crystalline) to banded spherulites at lower temperature, where both blocks were crystalline. The kinetics of crystallization were studied in detail via spherulite growth rates obtained from POM, and it was found that PPDX crystallization in the diblocks occurred much more slowly than in the homopolymers, this being responsible for the observed coincident crystallization of the two blocks during DSC cooling scans. On the other hand, the crystallized PPDX acts to nucleate the PCL block, so that heterogeneous crystallization was always observed even in copolymers containing a minority of this component (23%), for which "confined" crystallization might be expected. The crystallization kinetics of the PCL in the copolymers is accelerated by the presence of the crystalline PPDX block.

Introduction

The final solid-state structure in a semicrystalline block copolymer is the result of a complex interplay between microphase separation and crystallization. Three general cases have been described in the literature depending on the relative location of the order−disorder transition temperature, T_{ODT}, the glass transition temperature (T_g), and the crystallization temperature (T_c). In the first case, amorphous−crystallizable diblock copolymers that form a homogeneous melt are considered, where $T_{ODT} < T_c > T_g$, and microphase separation is driven by crystallization because of the low T_g of the amorphous block as compared to T_c of the crystallizable block. In this case a lamellar morphology results regardless of composition.[1−3] In the second case, weakly segregated systems with soft confinement have been described, where $T_{ODT} > T_c > T_g$. In this case the crystallization can provoke a "break-out" from the ordered melt morphology and crystallization can overwrite the morphological pattern of the melt with the possible formation of a lamellar structure once more regardless of composition.[3−7] The third general case is that of strongly segregated systems exhibiting hard confinement, where $T_{ODT} > T_g > T_c$. In this case, crystallization within spheres, cylinders, and other types of confined morphologies has been observed for diblock and triblock copolymers with one glassy block, and the microphase segregated structure of the melt is generally preserved.[7−14]

Polymer crystallization is usually preceded by heterogeneous nucleation, homogeneous nucleation, or self-nucleation. In bulk crystallizable polymers, nucleation is caused by heterogeneities (impurities, catalyst debris, or others). In block copolymers the nucleation depends on the continuity or isolation of the microdomains generated by phase segregation, since the number of heterogeneities could easily be much smaller than the number of isolated microdomains. Crystallization in continuous domains is induced by heterogeneous nucleation, because a percolation path for secondary crystallization exists. However, crystallization in isolated microdomains will either occur in a fractionated manner, where several crystallization exotherms are observed during a cooling DSC scan (the so-called fractionated crystallization phenomenon[8]), or can only be induced by homogeneous nucleation at extreme supercoolings.[8] In block copolymers where the crystallizable component is confined into cylinders or spheres, the number density of isolated microdomains can be far greater than the number of available heterogeneities, thus creating ideal conditions for homogeneous nucleation.[7,8]

When a crystallizable component is confined within a large number of small isolated microdomains, a substantial decrease in crystallinity compared to the corresponding homopolymers can sometimes be observed as a result of the larger supercoolings that are needed for crystallization and also topological restrictions due to confinement. Recently, several reports have shown a strong influence of confinement on crystalliza-

* Authors for correspondence.

10.1021/ma025766t CCC: $25.00
Published on Web 02/06/2003

tion kinetics.[7] If the crystallizable block is confined into spherical or cylindrical microdomains, an Avrami exponent of $n = 1$ has been observed and has been explained by homogeneous nucleation. However, in some puzzling cases Avrami exponents that are lower than 1 have been reported.[15,16]

In this work, the nucleation and crystallization of poly(*p*-dioxanone)-*b*-poly(ϵ-caprolactone) (P(PDX-*b*-CL)) diblock copolymers[17] are studied by means of optical microscopy, differential scanning calorimetry (DSC), and X-ray scattering. These novel AB diblock copolymers have interesting properties arising from the presence of two crystallizable components; additionally, they have potential applications as biodegradable and bioabsorbable materials. Bioabsorbable polymers degrade by hydrolytic processes within the human body, generally resulting in low-molecular-weight molecules, which can be metabolized or bioabsorbed by the body.[18,19] PPDX has been used as a biodegradable suture material.[20] PCL is also biodegradable; however, its hydrolytic degradation rate is much slower than that of PPDX. Therefore, using the diblock copolymer offers the possibility to control the deterioration of properties as a function of degradation time. Another interesting potential application is in the field of smart materials, where in this case a potential shape-memory function can be induced by specially designed heat treatments, as has been recently demonstrated for multiblock PPDX−PCL copolymers by Lendlein and Langer.[21]

Experimental Section

Materials. Toluene (Labscan, 99%) was dried by refluxing over calcium hydride and distilled just before use. 1,4-Dioxan-2-one (PDX, ca. 80%) was kindly provided by the Department of Chemical Engineering, Michigan State University. 20 g of crude PDX was first introduced in a previously flamed-dried two-necked round-bottom flask under a nitrogen flow and added with 200 mL of dry toluene. This solution was heated to 100 °C until complete dissolution and then cooled to 50 °C, and calcium hydride (Across, 93%) was added. After 24 h, toluene and PDX were successively distilled under reduced pressure (~10^{-1} mbar) by increasing the temperature from 40 to 140 °C. Purified PDX was finally recovered as a solid after toluene volatilization under reduced pressure and stored under a nitrogen atmosphere (yield = 80%). ϵ-Caprolactone (CL; Fluka, 99%) was dried over calcium hydride for 48 h at room temperature and distilled just before use. Aluminum triisopropoxide ($Al(O^iPr)_3$; Aldrich, 98%) was purified by distillation under reduced pressure and rapidly dissolved in dry toluene as previously described.[22] The accurate concentration of the initiator solution was determined by back complexometric aqueous titration of Al^{3+} with standard solutions of Na_2EDTA and $ZnSO_4$ at pH 4.8.[22] The polyesters denoted as PCL^{155} for a poly(ϵ-caprolactone) with a molar mass of 154 800 and $PPDX^{184}$ for a poly(1,4-dioxan-2-one) with an average viscosity molecular weight of 184 000 were respectively purchased from Aldrich and Johnson & Johnson (see Table 1).

Bulk Polymerization of 1,4-Dioxan-2-one (PDX). The bulk polymerization of PDX was carried out in a previously flamed-dried and nitrogen-purged 20 mL glass ampule equipped with a three-way stopcock capped with a rubber septum. The ampule was filled with 2.8 g of purified PDX (27.4 mmol), which was transferred in the melt state (T_m of PDX = 28 °C) through a previously flamed-dried stainless steel capillary under a nitrogen flow. Then, the ampule was thermostated in an oil bath at 80 °C before adding 0.40 mL of $Al(O^iPr)_3$ in toluene (concentration = 0.33 mol L^{-1}) with a syringe and stainless steel capillary. After a polymerization time of 7 min, the ampule was rapidly cooled to room temperature, and its content was dissolved in hot 1,2-dichloroethane. Poly(1,4-dioxan-2-one) (PPDX) was then selectively recovered by precipitation into 8 volumes of an ether−heptane (4:1) mixture, filtration, and drying under reduced pressure at 80 °C. Monomer conversion was determined by weighing the dried poly(ester-*alt*-ether) (conversion = 59%). After extraction of aluminum residues as described elsewhere,[17] the molar mass of $PPDX^5$ as denoted in Table 1 was determined by size exclusion chromatography with reference to polystyrene standards (M_n = 5500).

Table 1. Molecular Characteristics of the Materials Employed

composition[a]	M_n(PCL)	M_w/M_n	M_n(PPDX)	F_{PCL} (wt %)
$D_{23}{}^8C_{77}{}^{27}$	27 200	1.06	7 500	0.77
$D_{40}{}^4C_{60}{}^7$	7 100	1.17	4 800	0.60
$D_{77}{}^{32}C_{23}{}^{10}$	10 300	1.07	32 300	0.23
PCL^{11}	11 400	1.07		1.00
PCL^{55}	54 800	1.11		1.00
PCL^{98}	97 800	1.58		1.00
$PPDX^5$		1.24	5 500	0.00
$PPDX^{184}$			184 000	0.00

[a] D and C denote PPDX and PCL blocks, respectively; the superscripts are indicative of their molar masses (in thousands), and the subscripts refer to their weight fractions.

Solution Polymerization of ϵ-Caprolactone (CL). As previously reported by some of us,[17] the polymerization of ϵ-caprolactone (CL) was initiated by $Al(O^iPr)_3$ in toluene at 0 °C. Typically, 10 mL of CL (90.2 mmol) and 140 mL of toluene were introduced in a previously flamed-dried and nitrogen-purged round-bottom flask equipped with a three-way stopcock capped by a rubber septum. After thermostating at 0 °C, 1.30 mL of $Al(O^iPr)_3$ in toluene (concentration = 0.16 mol L^{-1}) was added, and the polymerization medium was vigorously stirred for 135 min. The poly(ϵ-caprolactone) (PCL) was then selectively recovered by precipitation in heptane, filtration, and drying. Monomer conversion was determined by weighing the polyester (conversion ≥ 99%). In a next step, aluminum residues were extracted according to a previously reported technique.[17] The molar mass of PCL^{55} as denoted in Table 1 was 54 800 as determined by size exclusion chromatography (SEC). Another poly(ϵ-caprolactone) sample denoted as PCL^{11} in Table 1 was obtained according to a similar procedure with a molar mass of 11 400 (see Table 1).

Synthesis of Poly(ϵ-caprolactone-*b*-1,4-dioxan-2-one) Block Copolymers (P(CL-*b*-PDX)). In a typical experiment, the polymerization of ϵ-caprolactone (2 mL, 18.0 mmol) in 14 mL of dry toluene was initiated by adding 1.60 mL of $Al(O^iPr)_3$ in dry toluene (concentration = 0.11 mol L^{-1}) at 0 °C in a previously flamed-dried and nitrogen-purged two-necked round-bottom flask equipped with a three-way stopcock capped with a rubber septum. After 1 h, 10.5 mL of the living poly(ϵ-caprolactone) (PCL) solution was picked out under a nitrogen flow, added with a few drops of HCl (0.1 M), poured into 8 volumes of heptane, and recovered by filtration and drying (conversion > 99%). Catalyst residues were removed out as described elsewhere,[17] and the molar mass was determined by size exclusion chromatography (M_n = 10 300). In a second step, the rest of the living PCL in toluene solution was added with 3.6 g (35.3 mmol) of purified PDX dissolved in 27 mL of dry toluene at room temperature through a stainless steel capillary and under a nitrogen atmosphere. After 43 h, the polymerization was stopped by adding of a few of drops of HCl (0.1 M). The poly(ϵ-caprolactone-*b*-1,4-dioxan-2-one) block copolymer (P(CL-*b*-PDX)) was recovered by precipitation into 8 volumes of heptane at room temperature, filtration, and drying under vacuum (conversion = 62%). Catalyst residues were extracted as previously reported.[17] The molar mass of PPDX block was determined by ^1H NMR spectroscopy from the relative intensities of methylene protons of the PDX repetitive units at 4.35 ppm and methylene protons of CL repetitive units at 2.32 ppm knowing the molar mass of the PCL macroinitiator ($M_{n,PPDX}$ = 32 200). The proportion between PDX and CL repetitive units also enabled to calculate weight fractions of 23% for PCL and 77% for PPDX. This sample is denoted $D_{77}{}^{32}$ $C_{23}{}^{10}$ in Table 1 where the capital letters refer

to PPDX and PCL blocks respectively, the superscripts are indicative of the molar mass (in thousands) and the subscripts indicate the weight fractions. Two other P(CL-*b*-PDX) block copolymers denoted as $D_{23}{}^{8}C_{77}{}^{27}$ and $D_{40}{}^{4}C_{60}{}^{7}$ in Table 1 were obtained according to a similar procedure.

Characterization. ^{1}H NMR spectra were recorded using a Bruker AMX-300 apparatus in $CDCl_3$. Size exclusion chromatography (SEC) of poly(ϵ-caprolactone) (PCL) and poly(1,4-dioxan-2-one) (PPDX) were performed respectively in THF at 35 °C and in $CHCl_3$ containing 0.3 wt % tri-*n*-octylmethylammonium chloride at 40 °C using a Polymer Laboratories (PL) liquid chromatograph equipped with a PL-DG802 degazer, an isocratic HPLC pump LC 1120 (flow rate = 1 mL/min), a Basic-Marathon autosampler, a PL-RI refractive index detector and three columns: a guard column PL gel 10 μm and two columns PL gel mixed-B 10 μm. Molecular weights and molecular weight distribution were calculated with reference to polystyrene standards. The absolute average-number molecular weight (M_n) of PCL were calculated by reference to a universal calibration curve and polystyrene standards in THF at 35 °C ($K_{PS} = 1.25 \times 10^{-4}$ dL/g, $a_{PS} = 0.707$; $K_{PCL} = 1.09 \times 10^{-3}$ dL/g, $a_{PCL} = 0.600$ in the $[\eta] = KM^a$, a Mark−Houwink relationship).

Polarized Optical Microscopy (POM). The superstructural morphology was observed in thin films prepared between microscope coverslips by melting the polymer at 130 °C for 10 min and then quickly cooling to the isothermal crystallization temperature in a hot-stage Linkam TP-91. The samples were placed between crossed polarizers in a Zeiss MC-80 optical microscope equipped with a camera system. To enhance contrast, a λ wave plate was inserted between the polarizers.

Differential Scanning Calorimetry (DSC). Samples of approximately 5 mg were encapsulated in aluminum pans and measured in a Perkin-Elmer DSC-7 calibrated with indium and cyclohexane under ultrapure nitrogen atmosphere. Two types of experiments were performed: standard and isothermal.

Standard DSC Experiments. In the standard DSC dynamic experiments, the samples were first heated to 130 °C in order to erase thermal history, and then a cooling run at 10 °C/min was recorded down to −20 °C, followed by a subsequent heating run performed also at 10 °C/min.

Isothermal DSC Experiments. In the isothermal crystallization experiments the diblock copolymer samples were subjected to two different experimental protocols in order to record the isothermal crystallization of both PPDX and PCL blocks simultaneously or just the crystallization of the PCL block:

(a) Simultaneous Isothermal Crystallization of PPDX and PCL Blocks. For the isothermal crystallization of both blocks, the sample was first heated to 130 °C to erase thermal history and then quickly cooled (at 80 °C/min) to the desired crystallization temperature where the isothermal DSC scan was recorded. Experiments were performed to ensure the samples did not crystallize during cooling to T_c by immediately heating the samples when the temperature reached the desired T_c; if any melting occurred, then it was concluded that crystallization took place during cooling and the isothermal experiment was not performed at that T_c (see Results and Discussion).

(b) Isothermal Crystallization of Only the PCL Block. In the case where only the crystallization of the PCL was recorded, the P(PDX-*b*-CL) diblock copolymer samples were first heated to 130 °C and then cooled at 10 °C/min down to −20 °C; during such cooling both blocks are able to crystallize (see below). Then the samples were heated to 62 °C and kept at that temperature for 70 min. At this temperature the PCL block was molten, but the PPDX block crystals could be annealed and some of the remaining amorphous fraction within the PPDX block could isothermally crystallize. Finally, the sample was quickly cooled (at 80 °C/min) to the desired crystallization temperature, and the isothermal DSC scan corresponding to the crystallization of the PCL block was recorded.

X-ray Scattering. Wide- and medium-angle X-ray scattering were performed on station 16.1 at the Synchrotron Radiation Source, Daresbury Lab, UK. The X-ray wavelength was $\lambda = 1.5$ Å. The samples were placed in TA Instruments DSC pans modified for transmission of X-rays by the insertion of mica windows. The pans were heated and cooled at 30 °C/min in a Linkam DSC of single-pan design. Diffraction patterns covering the scattering angle range 2θ(Cu Kα) = 4−23° were obtained using a Photonics Science CCD detector placed 215 mm from the sample. The two-dimensional images were compressed to 512 × 512 pixels for ease of data handling and were further reduced to one-dimensional profiles of intensity vs 2θ since no orientation was observed. The 2θ scale was calibrated using a HDPE reference sample and by "internal" calibration to the expected peak positions of crystalline PCL.

Results and Discussion

Before presenting our results, it is important to have an idea on the segregation strength and type of block copolymers that are being studied. These copolymers have only been recently prepared,[17] and there is little available data on their properties. One limitation of these block copolymers is their tendency to undergo hydrolytic degradation, in particular the PPDX block. Moreover, the thermal stability of PPDX is substantially lower than that of PCL so that the thermal degradation of PPDX is detectable above 150 °C. The investigation of the thermal decomposition behavior showed that the pyrolysis of PPDX mostly resulted in PDX formation.[23] Therefore, it was impossible to anneal the samples at high temperatures (i.e., in the melt) to try to obtain a better defined morphology, as is commonly done with block copolymers.

We have calculated the expected solubility parameters for the homopolymers employing the group contribution approximation proposed by Hoftyzer and Van Krevelen.[24] The results obtained are $\delta_{PCL} = 17.4$ J$^{1/2}$/cm$^{3/2}$ and $\delta_{PPDX} = 20.1$ J$^{1/2}$/cm$^{3/2}$. Even though the calculated parameters are not so different, PPDX and PCL do exhibit different solubility characteristics. For example, while PCL can dissolve at room temperature in many organic solvents including chloroform, methylene chloride, tetrahydrofuran, benzene, and toluene, PPDX is difficult to dissolve, and the best room temperature solvents available for this polymer are 1,1,2,2-tetrachloroethane and mixtures of phenol and 1,1,2,2-tetrachloroethane. PPDX is highly susceptible to hydrolytic degradation while PCL can also be hydrolyzed but at extremely slow rates under equivalent conditions.[25,26]

We have prepared blends of PPDX^{184} and PCL,^{98} and they were completely immiscible in the entire composition range explored according to the clear two-phase morphology (results not shown) observed by scanning electron microscopy (SEM). Additionally, in the paper by Raquez et al.[17] where the preparation of the copolymers employed here was first reported, the use of DSC clearly demonstrated the presence of two T_g transitions located at approximately −65 °C for the PCL block and −10 °C for the PPDX block. These T_g values coincide with the values of T_g for PPDX and PCL homopolymers; therefore, they confirm the immiscibility of the blocks, since not only their crystalline fractions are immiscible and do not form cocrystals, but their amorphous parts are also immiscible.

In view of all of the above, we consider PPDX and PCL to be immiscible and expect that the diblock copolymer will phase separate in the melt. A reasonable assumption was made that for the PPDX-*b*-PCL diblock copolymers, $T_{ODT} > T_c > T_g$, i.e., that the melt is microphase separated although crystallization occurs

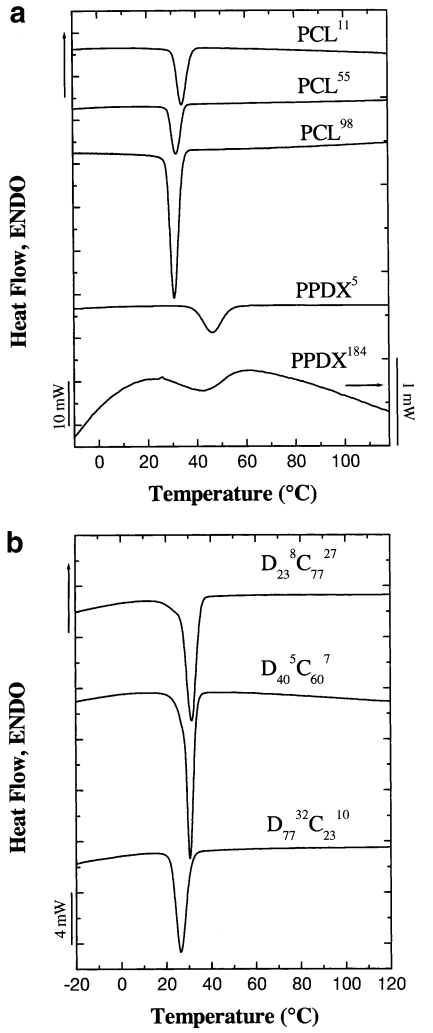

Figure 1. DSC cooling scans (10 °C/min) for (a) PCL and PPDX homopolymers of several molecular weights (see Table 1) and (b) P(PDX-*b*-CL) diblock copolymers.

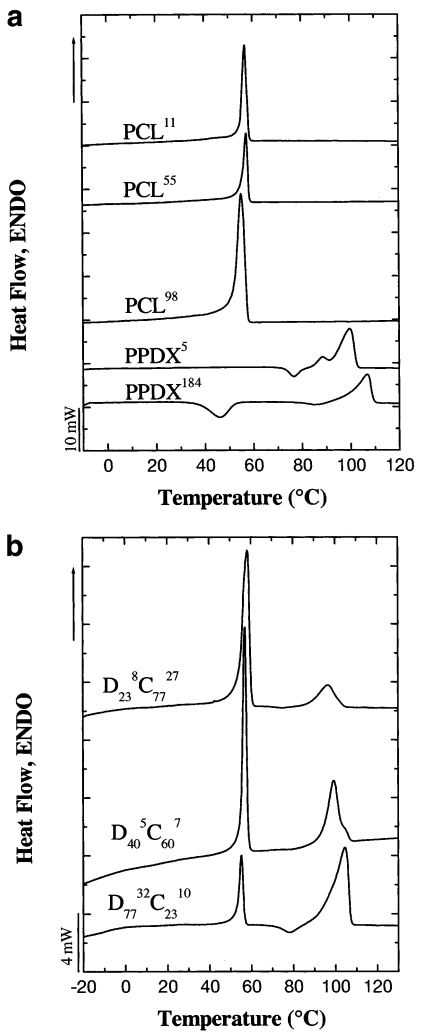

Figure 2. Subsequent heating DSC scans (10 °C/min) after the cooling shown in Figure 1 for (a) PCL and PPDX homopolymers of several molecular weights (see Table 1) and (b) P(PDX-*b*-CL) diblock copolymers.

under conditions of relatively soft confinement (since if one block crystallizes first, the softness of confinement changes with time). DSC heating scans were performed to try to detect the ODT temperature, but no change in the scan was detected up to 140 °C. Above that temperature, degradation started and any thermal events were masked by a vast baseline drift.

We were not able to obtain transmission electron microscopy images of any of the P(PDX-*b*-CL) diblock copolymers since the PPDX block is highly susceptible to degradation, and the samples deteriorated during attempts to stain them. SAXS indicated broad scattering peaks, with no discernible higher-order reflections, indicating the absence of long-range order.

Standard DSC Results. Figure 1 presents DSC cooling scans for a series of PPDX and PCL homopolymers and the three diblock copolymers studied while Figure 2 shows the subsequent heating scans. Table 2 lists all the relevant enthalpies and temperatures obtained from Figures 1 and 2. From the differences in peak crystallization temperatures between PCL and PPDX (31−34 °C for PCL and 44−47 °C for PPDX depending on the molecular weight), one would expect a clear distinction between the crystallization of each block in the P(PDX-*b*-CL) diblock copolymers, assuming that they are microphase separated and that they do not cocrystallize.

Figure 1b shows that regardless of diblock composition only one crystallization exotherm is observed, indicating that coincident crystallization has occurred at temperatures that are similar to those of PCL homopolymer or slightly lower (in the case of $D_{77}{}^{32}C_{23}{}^{10}$). The corresponding heating traces in Figure 2 show that each block is melting at temperatures that are similar to those of the corresponding homopolymers. A small decrease in melting temperature is observed on decreasing the fraction of either block. As the amount of PPDX in the block decreases from 77% to 23%, its melting point goes from 105 to 97 °C and in the case of PCL from 55 to 58 °C for equivalent compositions (see Table 2). Although this may be a consequence of morphological confinement, the effect is not very pronounced. Table 2 also shows that both blocks reached very substantial degrees of crystallinity (between 43 and 61%) with no particular trend with composition, a fact that may indicate lack of confinement.

One peculiar feature of PPDX homopolymers and PPDX blocks within P(PDX-*b*-CL) diblock copolymers is that they exhibit cold crystallization during heating.[27] Like many polyesters, PPDX does not crystallize completely during cooling, since the crystallization kinetics are not so fast. Then, when it is reheated at temperatures above T_g, it crystallizes before melting. In many

Table 2. DSC Derived Thermal Data of Homopolymers and Diblock Copolymers

	cooling scan		subsequent heating scan										
			PCL homopolymer or PCL block					PPDX homopolymer or PPDX block					
material	$T_{c,peak}$ (°C)	ΔH_c (J/g)	$T_{m,onset}$ (°C)	$T_{m,peak}$ (°C)	ΔH_m (J/g)	ΔH_m (J/g)[a]	% X_c PCL	$T_{c,peak}$ (°C)	ΔH_c (J/g)	$T_{m,onset}$ (°C)	$T_{m,peak}$ (°C)	ΔH_m (J/g)	ΔH_m (J/g)[a]	% X_c PPDX
PCL^{11}	34.1	−73.1	54.7	56.7	71.9	71.9	51.5							
PCL^{55}	32.9	−59.4	54.9	57.5	58.8	58.8	42.2							
PCL^{98}	30.8	−77.0		55.0	80.0	80.0	57.3							
$PPDX^{5}$	46.8	−64.7						76.7	−12.2	91.7	99.4	82.1	82.1	58.2
$PPDX^{184}$	43.8	−35.1						45.0/ 87.0	−17.4/ −5.2		106.8	58.3	58.3	41.3
$D_{23}{}^{8}C_{77}{}^{27}$	31.3	−61.2	54.3	58.2	54.5	70.8	50.8	75.4	−1.8	88.3	96.7	14.1	61.3	43.4
$D_{40}{}^{5}C_{60}{}^{7}$	30.5	−62.8	54.9	57.0	46.2	77.1	55.2	79.2	−1.3	93.7	99.2	34.2	85.6	60.6
$D_{77}{}^{32}C_{23}{}^{10}$	26.3	−52.6	53.0	55.2	17.1	74.2	53.2	77.8	−5.8	84.8	104.5	54.1	70.3	49.8

[a] Normalized values with respect to composition.

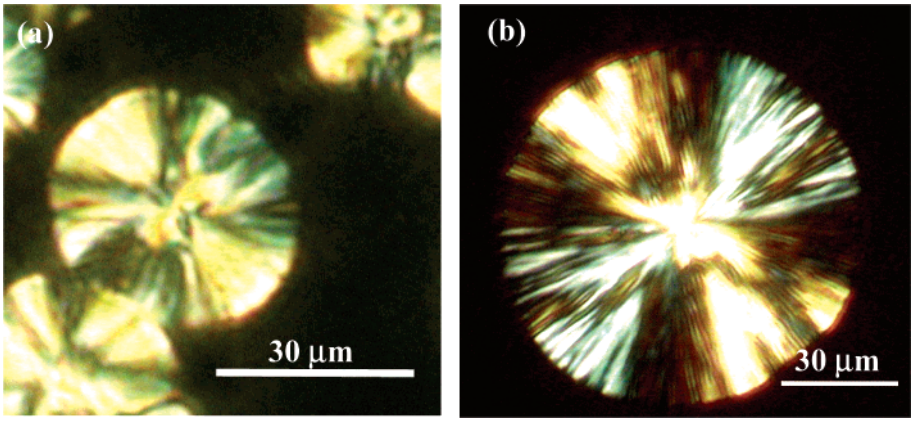

Figure 3. Polarized optical micrographs showing the spherulitic morphology of (a) PCL^{11} growing isothermally at 40 °C and (b) $PPDX^{5}$ growing isothermally at 62 °C.

cases reorganization during the heating DSC scan is also experienced by PPDX, and as a consequence, bimodal melting is observed (as for $PPDX^{5}$ in Figure 2a).[27]

According to Figure 1b, the PPDX block within P(PDX-*b*-CL) diblock copolymers always crystallizes at a lower temperatures than expected, and therefore its crystallization exotherm overlaps with that of the PCL block. If the crystallization enthalpies during cooling and heating, shown in Table 2, are balanced with the melting enthalpies, it can be seen that they match within the error of the measurements (about 20% depending on the quality of the baseline and the separation of exothermic and endothermic signals). This means that no significant crystallization occurs at lower temperatures (the runs were performed down to −20 °C) beyond the main coincident crystallization exotherm shown in Figure 1. In other words, it seems that fractionated crystallization of the PCL block does not occur even for the diblock whose PCL content is only 23%. This indicates that one of two possibilities pertains: (1) the morphology is arranged in such a way that a percolation path exists between the PCL phase (connected lamellae or cylinders, or a "break-out" morphology[7,8]), or (2) the PPDX crystallizes first (although at lower temperatures than it should) and therefore nucleates the PCL, a fact that could cause the observed coincident crystallization.[28] The isothermal crystallization experiments to be presented below as well as WAXS evidence indicate that possibility number two may be the correct mechanism responsible for the coincident crystallization observed regardless of composition in P(PDX-*b*-CL) diblock copolymers.

Polarized Optical Microscopy (POM). Both PCL and PPDX form well-defined spherulites that exhibit the classical Maltese-cross extinction pattern between crossed polars as can be seen in Figure 3.

In the case of P(PDX-*b*-CL) diblock copolymers spherulites were observed at high supercoolings, as evidenced in Figure 4; however, the superstructure changed to a granular aggregate morphology at lower supercoolings. Previous morphological examination of high molecular weight PPDX homopolymer also displayed qualitatively similar features, where well-defined PPDX spherulites were encountered at large and intermediate supercoolings, but at low supercoolings the superstructure changed to granular spherical aggregates.[27] However, Avrami indices obtained for $PPDX^{184}$ at temperatures where this granular spherical morphology is observed were close to 4, indicating three-dimensional superstructures growing from sporadic nuclei.[27]

For $D_{40}{}^{5}C_{60}{}^{7}$, the transformation to granular spherical aggregates started at 46 °C. For crystallization temperatures greater than 50 °C, PCL cannot crystallize, and the granular spherical aggregates observed correspond to the crystallization of just the PPDX block. Very similar results were obtained with the $D_{77}{}^{32}C_{23}{}^{10}$ diblock copolymer, where at very low supercooling, i.e., $T_c = 60$ °C, the granular aggregates that correspond to PPDX (the PCL block is molten at this temperature) exhibited an ellipsoidal shape that was apparently still three-dimensional since they showed a Maltese-cross pattern.

It is interesting to see in Figure 4a,b,f,g that the spherulites formed by the copolymers exhibited "banding". Banding is an extinction pattern observed between crossed polars and optically caused by a zero birefrin-

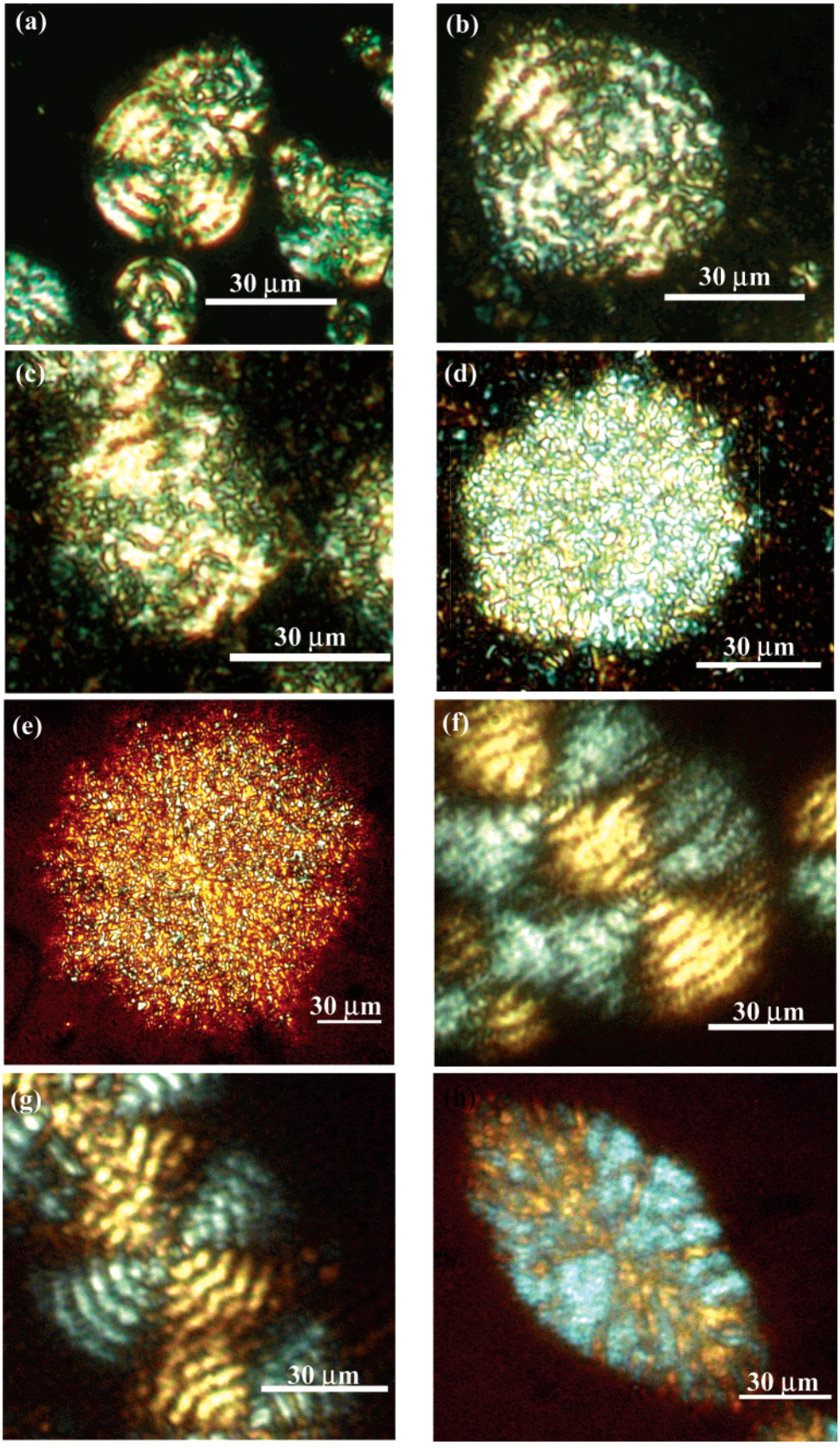

Figure 4. Polarized optical micrographs showing the superstructural morphology of PPDX-*b*-PCL diblock copolymer samples during isothermal crystallization: (a) $D_{40}{}^{5}C_{60}{}^{7}$, $T_c = 40$ °C; (b) $D_{40}{}^{5}C_{60}{}^{7}$, $T_c = 44$ °C; (c) $D_{40}{}^{5}C_{60}{}^{7}$, $T_c = 46$ °C; (d) $D_{40}{}^{5}C_{60}{}^{7}$, $T_c = 50$ °C; (e) $D_{40}{}^{5}C_{60}{}^{7}$, $T_c = 62$ °C; (f) $D_{77}{}^{32}C_{23}{}^{10}$, $T_c = 40$ °C; (g) $D_{77}{}^{32}C_{23}{}^{10}$, $T_c = 44$ °C; (h) $D_{77}{}^{32}C_{23}{}^{10}$, $T_c = 60$ °C.

gence effect.[29] Banding is physically produced by lamellar twisting during radial growth. The origin of lamellar twisting is still unclear, and several hypotheses have been postulated, including the accumulation of surface

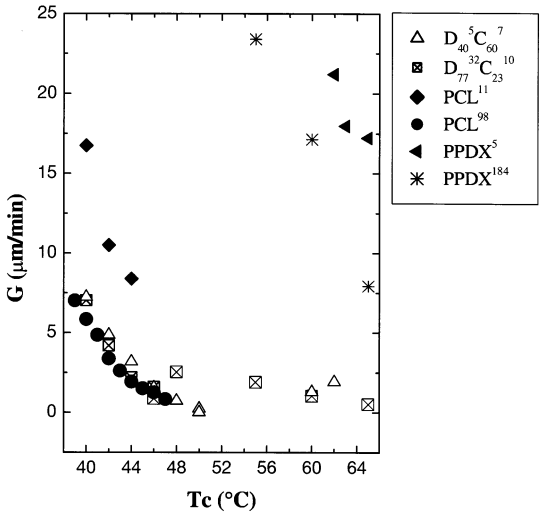

Figure 5. Superstructural growth rate as a function of isothermal crystallization temperature for the indicated samples.

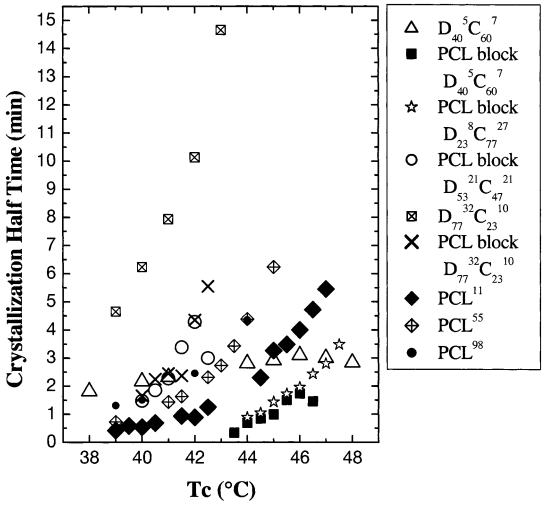

Figure 6. Experimental time required for 50% relative overall transformation (i.e., crystallization half-time) as a function of isothermal crystallization temperature for the indicated samples.

stress on the growing lamellar front.[30] High molecular weight PPDX exhibits "double" banding at high supercoolings.[27] On the other hand, it is well-known than PCL-containing block copolymers exhibit banding, as do blends of PCL with amorphous polymers.[31−33]

Both spherulites and granular spherical aggregates were followed as they grew with time at constant crystallization temperatures. In all cases linear plots of radii vs time were obtained, and thereby the superstructural growth rates were measured from the corresponding slopes. These are shown in Figure 5 as a function of crystallization temperature.

PPDX and PCL homopolymers exhibit a similar trend with molecular weight, as the M_n increases the spherulitic growth rate decreases (Figure 5). If the superstructural growth rate values (G) in Figure 5 are compared for the diblock copolymers $D_{40}{}^5C_{60}{}^7$ and $D_{77}{}^{32}C_{23}{}^{10}$ in the temperature range where both blocks crystallized (from 40 to 50 °C), it can be seen that they are very similar. The superstructural growth rate of the diblock copolymers is much lower than the growth rate of PPDX spherulites and even lower than PCL^{11} but comparable to that of PCL^{98}.

In the temperature range where PCL is molten, at T_c > 50 °C, the PPDX block within $D_{40}{}^5C_{60}{}^7$ and $D_{77}{}^{32}C_{23}{}^{10}$ diblock copolymers crystallizes at very slow rates compared to either of the PPDX homopolymer with distinct molecular weights. Figure 5 shows that the effect of having a molten PCL chain attached to it slows down the superstructural growth rate of the PPDX block by at least a factor of 10 as compared to PPDX homopolymers (at T_c > 50 °C). This is probably the reason why a coincident crystallization process is observed for P(PDX-*b*-CL) copolymers during a DSC cooling scan performed at 10 °C/min (Figure 1) regardless of composition. WAXS measurements were performed by quenching copolymer $D_{77}{}^{32}C_{23}{}^{10}$ from the melt to several crystallization temperatures, and the results clearly show that the PPDX block crystallizes first after an induction period, followed after a certain time by the crystallization of the PCL block (see below).

If the growth rate in Figure 5 is compared for the two copolymers examined in the temperature range where both blocks crystallized (in the range 40−50 °C), it can be seen that the superstructural growth rate is very similar for both copolymers.

Overall Crystallization Kinetics. The isothermal overall crystallization kinetics was studied by DSC. It must be remembered that such overall kinetic measurements include concurrent nucleation and crystallization of different portions of the system, and it will be referred to as transformation to semicrystalline state.[34] Initially, experiments that were analogous to those performed by POM were reproduced in the DSC, i.e., quenching from the melt, at temperatures where both blocks were molten, to the isothermal crystallization temperature. Since the crystallization kinetics of the two blocks overlapped, sometimes the isothermal crystallization exotherms were bimodal, indicating the superposition of two processes that were difficult to describe by a single Avrami equation. Therefore, we decided to measure the crystallization kinetics of the PCL block exclusively. To do this, we first crystallized the PPDX block, and only then was the temperature quickly lowered to T_c (see details in the Experimental Section).

The experimental time required for 50% relative overall transformation is plotted in Figure 6 for the homopolymers and the diblock copolymers. For $D_{40}{}^5C_{60}{}^7$ and $D_{77}{}^{32}C_{23}{}^{10}$ the data where the simultaneous transformation of both blocks was measured are also presented. It is interesting to compare these data with that for the transformation of only the PCL block after the PPDX block has been previously crystallized for the same copolymer. The results suggest that the crystallized PPDX block acts as a nucleating agent of the PCL block because its transformation rate within $D_{40}{}^5C_{60}{}^7$ or $D_{23}{}^8C_{77}{}^{27}$ is faster than PCL^{11} homopolymer over the range of T_c accessed. The simultaneous overall crystallization of both blocks within $D_{40}{}^5C_{60}{}^7$ and $D_{77}{}^{32}C_{23}{}^{10}$ is slower in view of the retardation of PPDX crystallization when it is covalently bonded to PCL (see previous section).

If a comparison is made among all the data where nucleation and crystallization of only PCL or PCL block were measured in Figure 6, it can be observed that the fastest transformations were obtained for PCL blocks within $D_{40}{}^5C_{60}{}^7$ and $D_{23}{}^8C_{77}{}^{27}$, where the PCL block is an excess component of the diblock copolymer and was nucleated by the previously crystallized PPDX. The PCL homopolymers crystallized somewhat slower than these copolymers, and their relative positions in Figure 6

depend on their molecular weights, where as expected the higher the M_n, the slower the transformation to the semicrystalline state. Finally, the material with the slowest transformation rate was $D_{77}{}^{32}C_{23}{}^{10}$.

It is interesting to consider the case of $D_{77}{}^{32}C_{23}{}^{10}$, since the PCL is a minor component and nevertheless it can crystallize at comparable supercoolings to PCL homopolymers. Especially after the PPDX block was allowed to crystallize first, one could envisage at least some intermediate confinement for the PCL block. Possibly as a result of such confinement its overall conversion rate is one of the slowest in Figure 6; nevertheless, the fact that it can crystallize at comparable supercoolings to PCL homopolymer excludes the possibility of homogeneous nucleation or fractionated crystallization.[7,8] The reason for such behavior could be that the already crystallized PPDX block provides the necessary nuclei for low supercooling crystallization.

One interesting observation that can be made in Figure 6 is that the data points do not encompass the same crystallization temperature range for all materials. The experiments are limited at high T_c by instrument resolution, i.e., if the crystallization kinetics is too slow, then the amount of heat evolved per unit time is too small to be registered. In the low T_c limit, on the other hand, the crystallization can be too fast, and the experiments are limited by crystallization during cooling to T_c; i.e., the sample could have already crystallized by a small amount before the isothermal DSC run starts, and this may lead to incomplete isothermal runs. We performed very careful tests to ensure that crystallization during cooling to T_c was not taking place, by doing an immediate melting run after reaching T_c and verifyng that no melting was obtained before running the actual isothermal crystallization experiment.

The isothermal overall crystallization of the samples where only the PCL block crystallizes was analyzed with the classical Avrami equation[30]

$$1 - v_c(t) = \exp[-Kt^n] \qquad (1)$$

where n is known as the Avrami index, K is the overall transformation rate constant (i.e., including nucleation and crystal growth), and $v_c(t)$ is the relative volume crystalline fraction of the polymer. The fit of the Avrami equation to the experimental data was very good (correlation coefficient 0.9999) up to a relative crystalline fraction of 45−50%. Beyond this transformation fraction, the experimental data deviated, possibly indicating that secondary crystallization processes were not described by a simple one-stage Avrami equation.[30] Two examples of Avrami fits to experimental data are provided in Figure 7. The fit for PCL^{11} is remarkably good in a very wide conversion range while in the case of the PCL block within $D_{77}{}^{32}C_{23}{}^{10}$ deviations occur at conversions characteristic of secondary crystallization. The difference in crystallization rate is apparent from the relative displacement in the time axis, and they are consistent with the half-crystallization time values discussed above and shown in Figure 6.

Figure 8 shows the variation of the overall transformation rate K as a function of crystallization temperature, and Figure 9 displays the equivalent trend of the Avrami index. Figure 8 corroborates the findings shown in Figure 6 as expected for good Avrami fits at 50% transformation fraction.

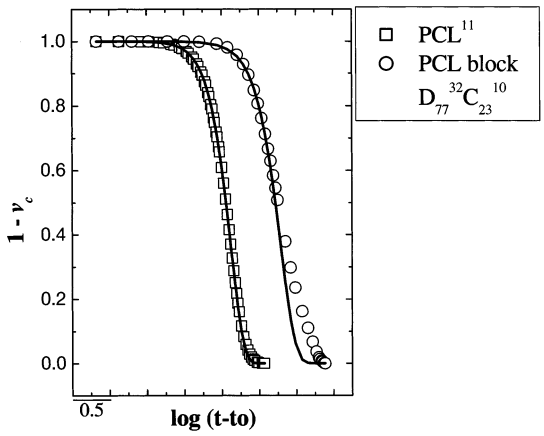

Figure 7. Crystallization isotherms at $T_c = 42$ °C where the relative amorphous fraction ($1 - v_c$) is plotted as a function of relative crystallization time (t in minutes) for a PCL homopolymer and for the PCL block within the indicated block copolymer (the PPDX block had been previously crystallized). The value of t_0 is the experimental time at which crystallization starts. The solid line represents the fit of the Avrami equation to the experimental data points.

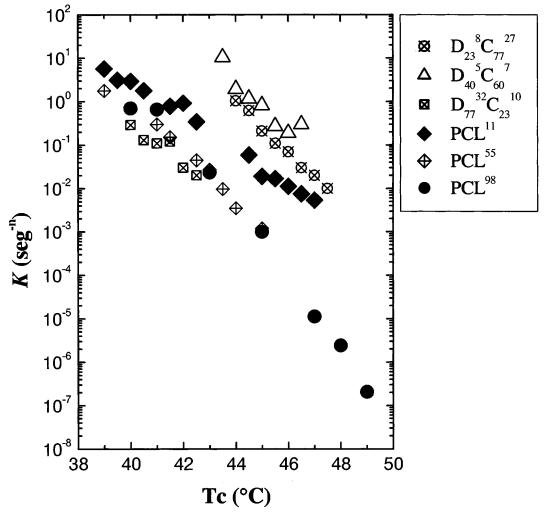

Figure 8. Overall crystallization rate constant, K, vs isothermal crystallization temperature for PCL homopolymers and for the PCL block within the indicated block copolymers (the PPDX block had been previously crystallized).

Figure 8 shows that the PCL blocks within $D_{40}{}^{5}C_{60}{}^{7}$ and $D_{23}{}^{8}C_{77}{}^{27}$ displayed a rather short crystallization range limited to high T_c temperatures. This is a consequence of their fast overall transformation rate probably caused by the nucleating effect of the already crystallized PPDX block. This is corroborated by the slower overall crystallization rate of the PCL homopolymers implicit not only in their K values but also in their much broader crystallization temperature range. The data for the PCL block within $D_{77}{}^{32}C_{23}{}^{10}$ is consistent with that of Figure 6.

In Figure 9, the usual trend of an increase in Avrami index with crystallization temperature is generally exhibited by most samples. The PCL homopolymers span a very wide range of n values, from $n = 2.4$ to $n = 4.4$, in a wide range of T_c, while the n values for the PCL block within the diblock copolymers are comparable to those of PCL^{55} and PCL^{11} across the T_c range. If a comparison is made at a specific T_c temperature, the PCL block within the copolymers has always a lower Avrami index than that of one of the PCL homopolymers

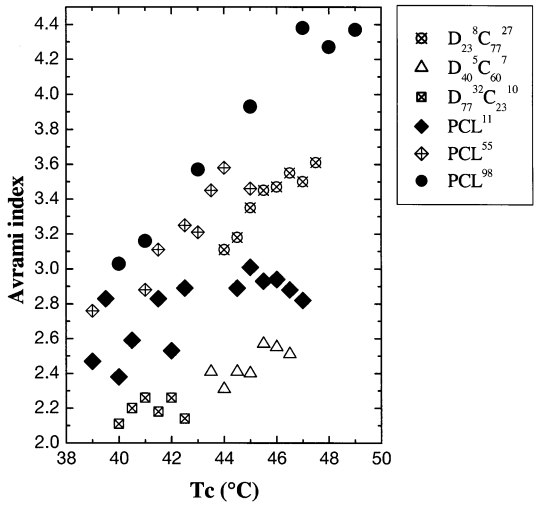

Figure 9. Avrami index, *n*, vs isothermal crystallization temperature for PCL homopolymers and for the PCL block within the indicated block copolymers (the PPDX block had been previously crystallized).

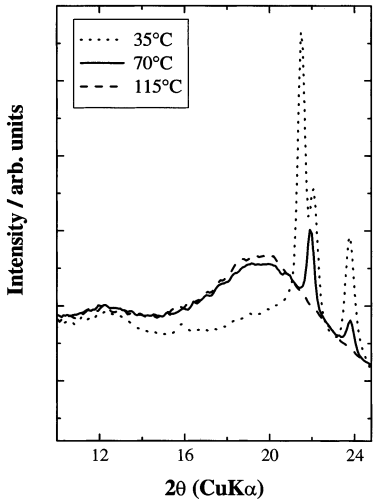

Figure 10. WAXS profiles obtained on heating $D_{40}{}^{5}C_{60}{}^{7}$ at the indicated temperatures.

of equivalent molecular weight. Furthermore, the value of the Avrami index decreases as the content of PCL in the diblock copolymer is reduced, a fact that may reflect the increasing morphological confinement of the PCL block. It is interesting to note that values of $n = 1$ were never encountered, another result that rules out homogeneous nucleation.[7] Even for the case where the PCL block represents only 23 wt % of the diblock copolymer the Avrami index varied between 2.1 and 2.3. This Avrami index close to 2 could correspond to two-dimensional crystals that are nucleated instantaneously or to one-dimensional crystals that are nucleated sporadically depending on the copolymer morphology.

X-ray Scattering. The contribution of PCL crystals to the wide-angle scattering patterns can fortunately be distinguished, since the first-order 110 reflection is quite well separated from the peaks from PPDX. Figure 10 shows data obtained on heating $D_{40}{}^{5}C_{60}{}^{7}$ from 35 to 115 °C. At 35 °C, both blocks are semicrystalline and contribute to the series of three sharp Bragg reflections, whereas at 70 °C, only PPDX is crystalline and the strongest Bragg reflection has disappeared. At approximately 100 °C the PPDX melts, and at higher temperatures, the WAXS pattern consists of a broad, diffuse peak due to amorphous polymer. Comparison of the WAXS profiles at 35 and 70 °C enables the contributions from PPDX and PCL to be resolved. The first reflection at $2\theta = 21.5°$ corresponds to the first-order 110 reflection from PCL,[35] while the second reflection at 22.0° corresponds to a superposition of the second-order 111 reflection from PCL ($2\theta = 22.05°$) and the first-order reflection from PPDX ($2\theta = 21.96°$). Similarly, the third-order peak at $2\theta = 23.8°$ contains contributions from both PCL and PPDX.[36] In the following analysis of the WAXS data, the intensities under these three peaks as well as the diffuse amorphous peak were determined using an automated peak fitting routine (xfit from the CCP13 suite[37]) with the appropriate number of Gaussians. A fourth-order polynomial background was fixed using parameters obtained by fitting the first (or last) frame. Because of difficulties in estimating the contribution from background scattering compared to the amorphous peak, the latter should be regarded as relative values. Consequently, the degree of crystallinity estimated from the sum of the relative areas of crystalline Bragg peaks compared to the total area under the diffuse amorphous and crystalline peaks is also only a relative quantity.

To investigate the influence on PCL crystallization due to confinement by crystalline PPDX on $D_{40}{}^{5}C_{60}{}^{7}$, a series of quenches were performed starting at $T = 65$ °C where PCL was molten and quenching to $T_c = 45$, 40, or 35 °C, where PCL crystallizes. The samples were heated to 65 °C at 30 °C/min and held at that temperature for a brief period of time (1−5 min) before cooling (also at 30 °C/min) to the crystallization temperature. It is important to point out that the time spent at 65 °C has an effect on the PCL block crystallization kinetics, since at that temperature the PPDX crystals can anneal and the remaining amorphous part of the PPDX block can crystallize. Separate DSC experiments confirmed that the time spent at 65 °C influences the subsequent crystallization times of the PCL block. The higher the starting crystallinity of the PPDX block, the faster the crystallization kinetics of the PCL block. In view of this effect, the crystallization kinetic measurements obtained by WAXS are not directly comparable to those presented above (Figure 6).

The WAXS data were analyzed to determine the areas under the crystalline and amorphous peaks as well as the relative degree of crystallinity. The corresponding data are shown in Figure 11. Inspection of this figure enables a number of conclusions to be drawn. First, the onset of crystallization is delayed significantly at 45 °C, compared to the two deeper quenches, although this temperature is well below the melting temperature for homopolymer PCL. Second, at 45 °C the crystallization is very weak, as shown by the relative intensity of the PCL crystal peak (at $2\theta = 21.5°$) and by the fact that the intensities of the higher-order peaks do not change substantially, showing that they are dominated by contributions from the already-crystalline PPDX. Finally, we note that for the deeper quenches the degree of crystallinity follows the crystallization of PCL.

We now discuss WAXS data obtained for sample $D_{77}{}^{32}C_{23}{}^{10}$. This contains 77% PPDX compared to 40% for $D_{40}{}^{5}C_{60}{}^{7}$. This is reflected in the WAXS pattern shown in Figure 12, where the peak at $2\theta = 21.5°$ from PCL is now a shoulder on the strongest peak at $2\theta = 22°$, arising predominantly from PPDX. On heating, melting of PCL is observed before PPDX for $D_{77}{}^{32}C_{23}{}^{10}$,

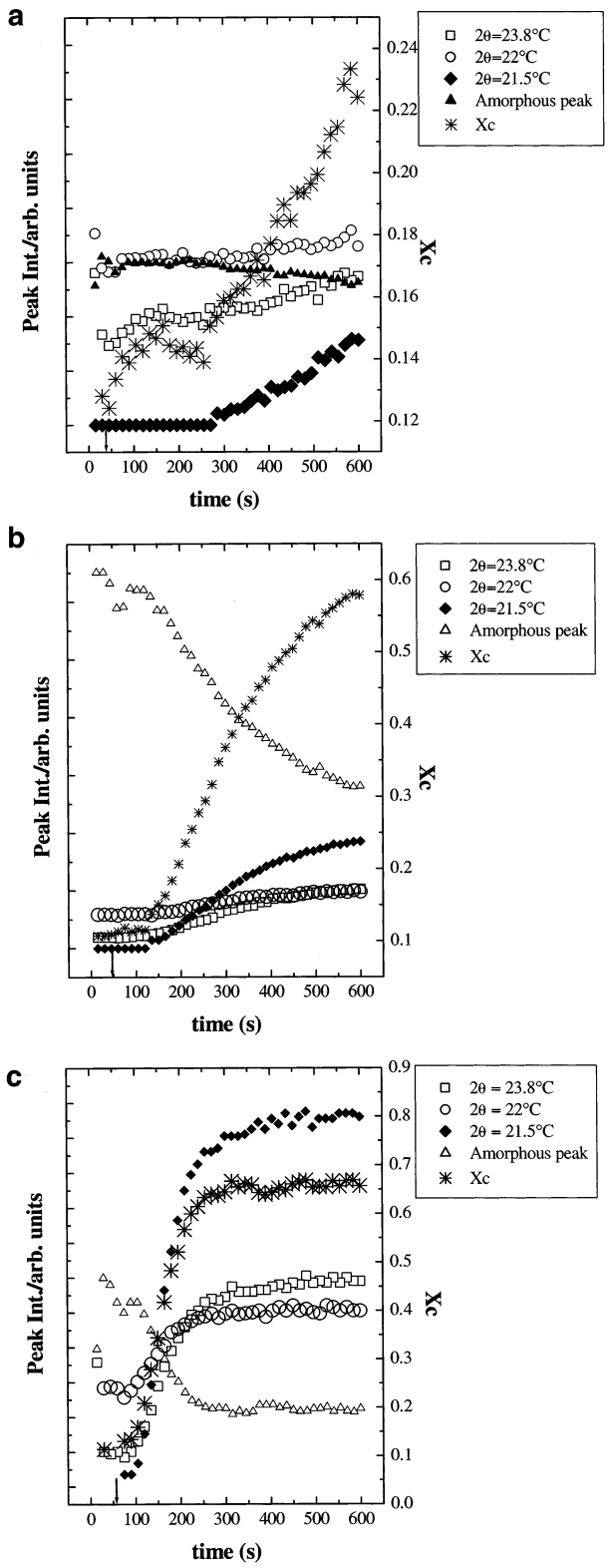

Figure 11. Relative integrated intensities under the peaks (left scales, see legend) and relative degree of crystallinity (right scale) obtained from WAXS data for $D_{40}{}^{5}C_{60}{}^{7}$ quenched from $T = 65$ °C to (a) 45 °C, (b) 40 °C, (c) 35 °C. The cooling rate was 30 °C/min. The arrows indicate the nominal points at which the final temperature was reached. For convenience, in (a) the amorphous peak intensity has been divided by 10 and in (c) by 5.

as for $D_{40}{}^{5}C_{60}{}^{7}$, as shown by the WAXS data in Figure 12.

For sample $D_{77}{}^{32}C_{23}{}^{10}$, WAXS experiments were performed to monitor changes in the crystal structure on

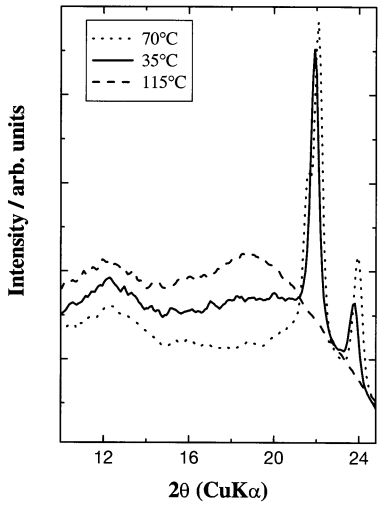

Figure 12. WAXS profiles obtained on heating $D_{77}{}^{32}C_{23}{}^{10}$ at the indicated temperatures.

quenching from the melt at $T = 115$ °C to temperatures $T = 40$, 30, and 25 °C, below T_m (PCL). In this case crystallization of both blocks is expected. The aim was to investigate which block was crystallizing first, since the DSC results presented in Figure 1 indicated a coincident crystallization phenomenon upon cooling from the melt at a rate of 10 °C/min.

Figure 13 shows results from analysis of the integrated WAXS peak areas as well as the relative degree of crystallinity determined from the WAXS data. Figure 13a shows that for the shallowest quench, to $T_c = 40$ °C, the PCL does not crystallize within the time scale investigated since no peak at $2\theta = 21.5°$ was observed. The degree of crystallinity of the PPDX increases during the course of isothermal annealing, and the amorphous peak area decreases, reaching a plateau upon completion of crystallization. In contrast, it is evident from Figure 13b,c that two-stage crystallization occurs. First the peaks at $2\theta = 22°$ and 23.5° grow, reaching a plateau prior to a further increase in integrated area upon PCL crystallization. The PCL crystallization is most clearly seen in the growth of the $2\theta = 21.5°$ peak after an induction time, which decreases with increasing quench depth (from 270 s at $T_c = 30$ °C to 230 s at $T_c = 25$ °C). It should be noted that due to difficulties mentioned above in separating the background from the amorphous peak area, the degrees of crystallinity are on a relative scale for each data set and cannot be compared from one data set to another.

The results presented above for copolymer sample $D_{77}{}^{32}C_{23}{}^{10}$ support the previously presented DSC evidence that points to a nucleating effect of PPDX on PCL, since they have helped to establish that even under isothermal conditions the PPDX block crystallizes first, closely followed by the PCL block.

In a related previous work, Bodganov et al.[38] studied by DSC the isothermal crystallization of three different types of poly(ϵ-caprolactone-*co*-ethylene glycol) block copolymers (PCL-*b*-PEG) with varying molecular architectures: A−B, $(A)_2$−B, and A−B−A. They found that the PCL always crystallized first and that the crystallization rate of the PEG component was retarded as compared to an equivalent homopolymer. They attributed this growth retardation to the mutual influence between the PEG constituent and the PCL crystal phase which hardens the total copolymer structure.

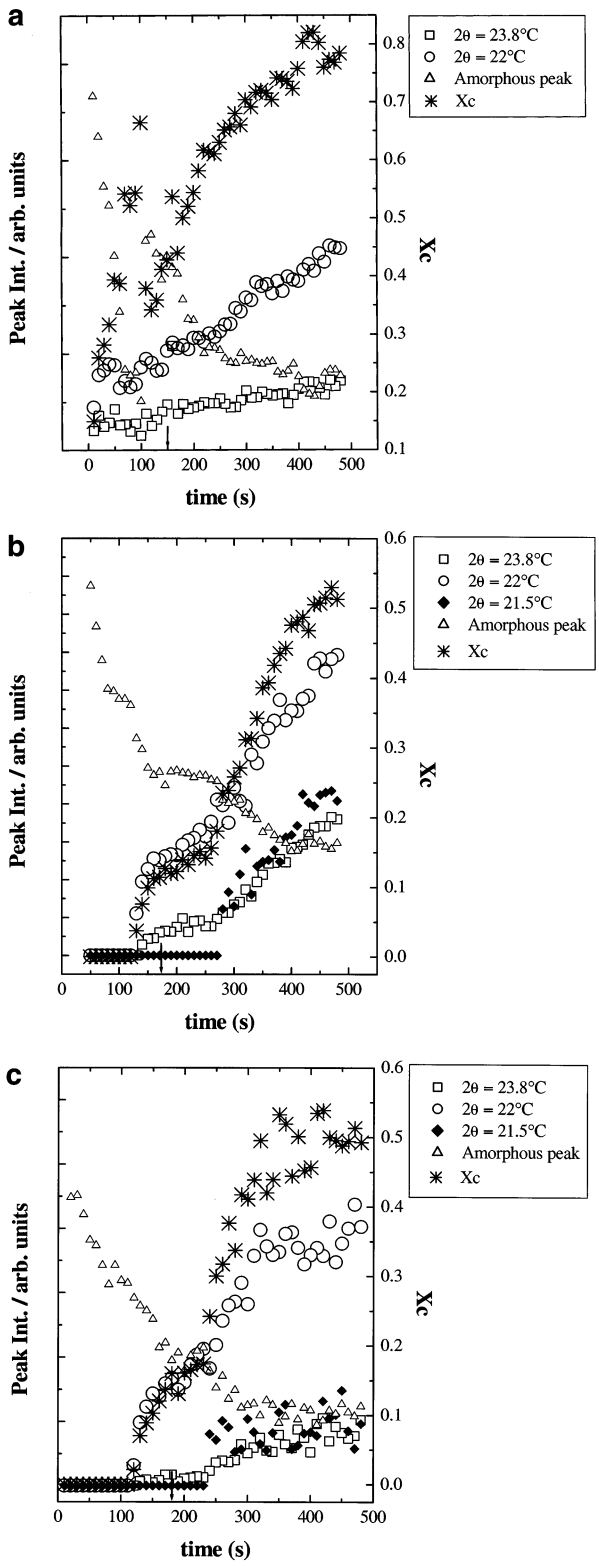

Figure 13. Relative integrated intensities under the peaks (left scales, see legend) and relative degree of crystallinity (right scale) obtained from WAXS data for $D_{77}{}^{32}C_{23}{}^{10}$ quenched from $T = 115$ °C to (a) 40 °C, (b) 30 °C, (c) 25 °C. The cooling rate was 30 °C/min. The arrows indicate the nominal points at which the final temperature was reached. For convenience, the amorphous peak intensity has been divided by 5 in (a)–(c).

Conclusions

The crystallization and morphology of novel P(PDX-*b*-CL) diblock copolymers have been studied by DSC, WAXS, and POM. The copolymers exhibit banded spherulitic superstructures that progressively changed to spherical granular aggregates at lower supercoolings. The crystallization of the PPDX block within the block copolymers is very slow as compared to that of PPDX homopolymer. This slow crystallization kinetics causes a coincident crystallization phenomenon when the copolymer is cooled from the melt in the DSC.

The WAXS and DSC results indicate that, during isothermal crystallization in a supercooling range where both blocks can crystallize, the PPDX crystallizes first and nucleates the PCL block. This nucleation effect can explain the lack of fractionated crystallization in PCL regardless of composition, even when it only amounts to 23 wt % in the diblock copolymer. In experiments where the PPDX block is first crystallized fully before the PCL block is isothermally crystallized, it was shown how the overall crystallization kinetics of the PCL block is accelerated by the nucleation effect induced by the already crystallized PPDX, in such a way that the transformation to the semicrystalline state is faster for the PCL block of certain copolymers than for PCL homopolymers.

Acknowledgment. The Simón Bolívar University team acknowledges sponsorship by Fonacit through Grant S1-2001000742. V.C. and I.W.H. thank the EPSRC (UK) for financial support, Anthony Gleeson for assistance in the X-ray scattering experiments, and the CCP13 initiative (UK) for provision of software used to analyze the WAXS data, in particular to G. Rajkumar (Raj) (Imperial college) for the conversion routine for tiff files. LPCM members thank the Service Fédéraux des Affaires Scientifiques, Techniques et Culturelles in the frame of the PAI-5/03, as well as the Région Wallonne and Fonds social Européen in the frame of the Materia Nova program, for general support. J-M. Raquez is grateful to F.R.I.A. for his PhD grant.

References and Notes

(1) Rangarajan, P.; Register, R. A.; Adamson, D. H.; Fetters, L. J.; Bras, W.; Naylor, S.; Ryan, A. J. *Macromolecules* **1995**, *28*, 1422.
(2) Ryan, A. J.; Hamley, I. W.; Bras, W.; Bates, F. S. *Macromolecules* **1995**, *28*, 3860.
(3) Richardson, P. H.; Richards, R. W.; Blundell, D. J.; MacDonald, W. A.; Mills, P. *Polymer* **1995**, *36*, 3059.
(4) Hamley, I. W.; Patrick, J.; Fairclough, A.; Terrill, N. J.; Ryan, A. J.; Lipic, P. M.; Bates, F. S.; Towns-Andrews, E. *Macromolecules* **1996**, *29*, 8835.
(5) Nojima, S.; Kato, K.; Yamamoto, S.; Ashida, T. *Macromolecules* **1992**, *25*, 2237.
(6) Ryan, A. J.; Fairclough, J. P. A.; Hamley, I. W.; Mai, S.-M.; Booth, C. *Macromolecules* **1997**, *30*, 1723.
(7) Loo, Y.-L.; Register, R. A.; Ryan, A. J. *Macromolecules* **2002**, *35*, 2365 and references therein.
(8) Müller, A. J.; Balsamo, V.; Arnal, M. L.; Jakob, T.; Schmalz, H.; Abetz, V. *Macromolecules* **2002**, *35*, 3048 and references therein.
(9) Nojima, S.; Toei, M.; Hara, S.; Tanimoto, S.; Sasaki, S. *Polymer* **2002**, *43*, 4087.
(10) Reiter, G.; Castelein, G.; Sommer, J.-U.; Röttele, A.; Thurn-Albrecht, T. *Phys. Rev. Lett.* **2001**, *87*, 226101.
(11) Arnal, M. L.; Balsamo, V.; López-Carrasquero, F.; Contreras, J.; Carrillo, M.; Schmalz, H.; Abetz, V.; Laredo, E.; Müller, A. J. *Macromolecules* **2001**, *34*, 7973.
(12) Zhu, L.; Cheng, S. Z. D.; Calhoun, B. H.; Ge, Q.; Quirk, R. P.; Thomas, E. L.; Hsiao, B. S.; Yeh, F.; Lotz, B. *Polymer* **2001**, *42*, 9121.
(13) Weimann, P. A.; Hajduk, D. A.; Chu, C.; Chaffin, K. A.; Brodil, J. C.; Bates, F. S. *J. Polym. Sci., Part B: Polym. Phys.* **1999**, *37*, 2053.

(14) Chen, H.-L.; Hsiao, S.-C.; Lin, T.-L.; Yamauchi, K.; Hasegawa, H.; Hashimoto, T. *Macromolecules* **2001**, *34*, 671.
(15) Lotz, B.; Kovacs, A. J. *Polym. Prepr. (Am. Chem. Soc., Div. Polym. Chem.)* **1969**, *10*, 820.
(16) Shiomi, T.; Tsukada, H.; Takeshita, H.; Takenaka, K.; Tezuka, Y. *Polymer* **2001**, *42*, 4997.
(17) Raquez, J.-M.; Degée, P.; Narayan, R.; Dubois, P. *Macromol. Rapid Commun.* **2000**, *21*, 1063.
(18) Williams, D. *J. Mater. Sci.* **1982**, *17*, 1233.
(19) Karlsson, S.; Hakkarainen, M.; Albertsson, A. C. *J. Chromatogr.* **1994,** *688*, 251.
(20) Chu, C. C. *J. Appl. Polym. Sci.* **1981**, *26*, 1727.
(21) Lendlein, A.; Langer, L. *Science* **2002**, *296*, 1673.
(22) Ropson, N.; Dubois, P.; Jérôme, R.; Teyssié, P. *J. Polym. Sci., Polym. Chem. Ed.* **1997**, *35*, 183.
(23) Nishida, H.; Yamashita, M.; Endo, T. *Polym. Degrad. Stab.* **2002**, *78*, 129.
(24) Van Krevelen, D. W. *Properties of Polymers*, 3rd ed.; Elsevier: Amsterdam, 1997.
(25) Sabino, M. A.; Feijoo, J. L.; Müller, A. J. *Polym. Degrad. Stab.* **2001**, *73*, 541.
(26) Li, S.; Garreau, H.; Vert, M.; Petrova, T.; Manolova, N.; Rashkov, I. *J. Appl. Polym. Sci.* **1998**, *68*, 989.
(27) Sabino, M. A.; Feijoo, J. L.; Müller, A. J. *Macromol. Chem. Phys.* **2000**, *201*, 2687.
(28) Manaure, A.; Müller, A. J. *Macromol. Chem. Phys.* **2000**, *201*, 958.
(29) Wunderlich, B. *Macromolecular Physics*; Academic Press: New York, 1980; Vol. 1.
(30) Gedde, U. W. *Polymer Physics*; Chapman and Hall: London, 1995.
(31) Balsamo, V.; von Gyldenfeldt, F.; Stadler, R. *Macromol. Chem. Phys.* **1996**, *197*, 3317.
(32) Hernández, M. C.; Laredo, E.; Bello, A.; Carrizales, P.; Marcano, L.; Balsamo, V.; Grimau, M.; Müller, A. J. *Macromolecules* **2002**, *35*, 7301.
(33) Keith, H. D.; Padden, F. J.; Russell, T. P. *Macromolecules* **1989**, *22*, 666.
(34) Schultz, J. *Polymer Crystallization*; American Chemical Society: Washington, DC, 2001.
(35) Chatani, Y.; Okita, Y.; Tadokoro, H.; Yamashita, Y. *Polym. J.* **1970**, *1*, 555.
(36) Kricheldorf, H. R.; Damrau, D. *Macromol. Chem. Phys.* **1998**, *199*, 1089.
(37) http://www.ccp13.ac.uk.
(38) Bogdanov, B.; Vidts, A.; Schacht, E.; Berghmans, H. *Macromolecules* **1999**, *32*, 726.

MA025766T